INSTITUTE OF PHYSICS PUBLISHING JOURNAL OF PHYSICS D: APPLIED PHYSICS

J. Phys. D: Appl. Phys. **36** (2003) 775–778 PII: S0022-3727(03)57941-4

Microstructure and magnetic properties of $Nd_{60}Al_{10}Fe_{20}Co_{10}$ glass-forming alloy

Lei Xia[1,2], Bing Chen Wei[3], Zhi Zhang[2], Ming Xiang Pan[2], Wei Hua Wang[2,4] and Yuan Da Dong[1]

[1] Institute of Material, Shanghai University, Shanghai 200072, People's Republic of China
[2] Institute of Physics, Chinese Academy of Science, Beijing 100080, People's Republic of China
[3] National Microgravity Laboratory, Institute of Mechanics, Chinese Academy of Science, Beijing 100080, People's Republic of China

E-mail: whw@aphy.iphy.ac.cn

Received 8 January 2003
Published 19 March 2003
Online at stacks.iop.org/JPhysD/36/775

Abstract

The microstructural variations of the $Nd_{60}Al_{10}Fe_{20}Co_{10}$ melt-spun ribbons and the as-cast rod were studied by high resolution transmission electron microscopy (HRTEM), x-ray diffraction (XRD) and differential scanning calorimetry. Nano-clusters in glassy matrix in both melt-spun ribbon and the as-cast rod samples were observed by HRTEM, though no obvious crystalline reflections were displayed in either the XRD or selected area electron diffraction patterns. The magnetic properties of the rod sample were compared to that of the ribbons. It was found that the coercivity of the alloy increases with the size of the nano-scaled clusters, while the cluster size increases with the reduction of cooling rate at which the sample were prepared. The relationship between the microstructure and magnetic and thermal properties of the Nd based alloy were discussed by random anisotropy model.

1. Introduction

Metallic glasses have evoked intensive interest since 1960s because they exhibit some properties superior to their crystalline counterparts [1–10]. Recently, Nd(Pr)–Fe based bulk metallic glasses (BMGs) prepared in various methods have been reported and a lot of research work has been done on them due to their unique magnetic properties and the absence of glass transition temperature before crystallization in differential scanning calorimetry (DSC) measurements [11–19]. It is found that the Nd-rich BMGs exhibit a high coercivity while the melt-spun ribbons of the same composition has a much lower coercivity though both of them exhibit similar crystallization behaviour. Previous work mostly focused on these facts and some theoretical presumptions. It is assumed that a relaxed structure of assembled Nd(Pr)–Fe or Nd(Pr)–Fe–Al clusters with large random magnetic anisotropy (RMA), which responds to the hard magnetic properties, exist in the Nd-rich BMGs, and the microstructure and the coherence length of amorphous alloy may change with the quenching rate [14, 15, 17, 21, 22]. However, no direct evidences have been found to support these presumptions, and the relationship between microstructure and magnetic properties is still unclear. In this paper, the $Nd_{60}Al_{10}Fe_{20}Co_{10}$ alloy in melt-spun ribbons obtained at different cooling rates and suction-cast cylindrical samples with a diameter of about 3 mm were used. The microstructure of the ribbon and rod samples and their magnetic properties were studied. The formation of the clusters as well as their relationship to the magnetic properties was discussed.

2. Experimental procedure

Ingots with a nominal composition of $Nd_{60}Al_{10}Fe_{20}Co_{10}$ were prepared by arc-melting of elements Nd, Fe, Al and Co with the purity of 99.9 at% in a titanium-gettered argon atmosphere. Ribbons were obtained by melt-spinning using a single copper wheel with surface speeds from about 3 to 15 m s^{-1} under pure argon atmosphere. As-cast rod samples were taken from the central region of a cylinder of 3 mm in

[4] Author to whom correspondence should be addressed.

diameter and 80 mm in length prepared by suction casting under pure argon atmosphere. The structure of the samples was characterized by x-ray diffraction (XRD) in a Philips diffractometer using CuK_α radiation. The element distribution and the composition of the samples were detected by a NORAN VANTAGE energy dispersive spectrometer (EDS). The microstructure of the samples was observed on a JEOL JEM-2010 high resolution transmission electron microscope (HRTEM). Specimens for HRTEM observation were thinned under pure argon atmosphere on a rotating plate cooled by liquid nitrogen. A vibrating sample magnetometer (VSM) was used for the magnetic measurements of the as-cast rod and as-spun ribbons. DSC measurements were carried out under a purified argon atmosphere in a Perkin Elmer DSC-7 at a heating rate of 0.17 K s^{-1}. The calorimeter was calibrated for temperature and energy at various heating rates with high purity indium and zinc. An empty Al pan was firstly scanned to establish a baseline, then a measurement with the same Al pan including the sample was carried out again at the identical thermal condition.

3. Results

The composition of $Nd_{60}Al_{10}Fe_{20}Co_{10}$ as-cast sample and melt-spun ribbons is proved to be homogeneous within the EDS detection limit. XRD patterns in figure 1 shows the typical broad diffraction maxima of amorphous phase for both as-cast rod sample and as-spun ribbon, and no obvious crystalline peaks were found. By careful examination, however, slightly splitting of brief maximum exists for rod sample, as shown in figure 1(a). It suggests that there might be a small amount of nanocrystals or clusters present in the samples [13].

Figure 2 shows the DSC curves of melt-spun ribbons with the wheel speeds of 3, 9, 12 and 15 m s^{-1} and the as-cast rod. A sharp exothermic peak followed closely by an endothermic peak was found in all DSC curves. The sharp exothermic reaction is confirmed to be the main crystallization process and the endothermic one represents the melting behaviour. A weak exothermic peak at about 473 K appears in the curves of melt-spun ribbons at the wheel speeds above 9 m s^{-1}. The peak becomes weaker with the decreasing of cooling rate and disappears in the curves of 3 m s^{-1} wheel-speed ribbon and the 3 mm rod, while the main crystallization peak temperature moves to higher point. This paper has proved that this weak exothermic peak corresponds to the formation of nanocrystals that are closely related to the high coercivity of the alloy. It should be noticed that all the five samples have almost the same crystallized equilibrium phase, the same composition and the nearly same melting temperature.

HRTEM images of the as-cast rod and the melt-spun ribbon at a wheel speed of 15 m s^{-1} are shown in figure 3. There are a large number of isolated clusters distributed randomly in the amorphous matrix with the size ranging from 3 to 6 nm in the as-cast rod sample. The clusters are too small to be reflected in the selected area diffraction pattern (SADP) even in the cluster-abundant area, as shown in the inset of figure 3(*a*). The interplanar distance of the cluster is a uniform 0.273 nm. In contrast, figure 3(*b*) displays the HRTEM image of the melt-spun ribbon at a wheel speed of 15 m s^{-1}. The selected area electron diffraction pattern in the inset of figure 3(*b*) demonstrates the bulk amorphous characteristics. However, many isolated clusters with an average size scale of 1–2 nm can also be found embedded in the glassy matrix, but not as regular as these in the rod sample. The size of clusters in both rod and ribbon samples agrees well with the results of the magnetic force microscopy (MFM) observation [18, 22].

The profile of hysteresis loops of $Nd_{60}Al_{10}Fe_{20}Co_{10}$ as-spun ribbons at different wheel speeds and as-cast rod is shown in figure 4. The coercivity (H_c) reaches about 330 kA m^{-1} in the rod sample, but decreases gradually from 180 to 30.5 kA m^{-1} with the increase of wheel speed (i.e. quenching rate) from 3 to 18 m s^{-1} in the ribbons. The saturation magnetization (σ_s) under external field of 1432 kA m^{-1} and remanent magnetization (σ_r) also decrease subsequently from as-cast rod to the ribbons with increasing wheel speed. These results are in accordance with those of other Nd–Fe based metallic glass systems [14, 18, 21, 22].

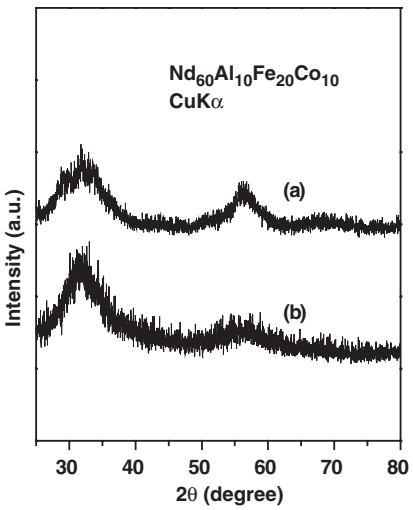

Figure 1. The XRD patterns of $Nd_{60}Al_{10}Fe_{20}Co_{10}$ alloys: (a) rod of 3 mm in diameter and (b) ribbon with a wheel speed of 15 m s^{-1}.

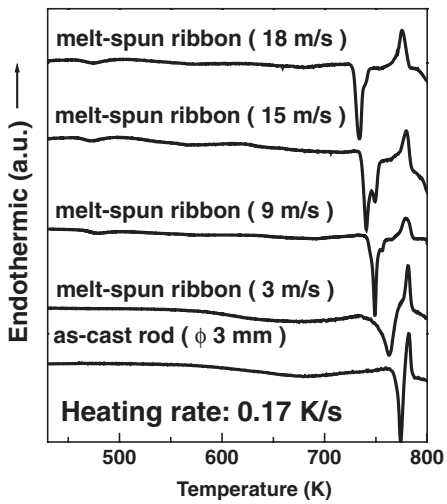

Figure 2. DSC traces of as-cast rod of 3 mm in diameter and as-spun ribbons melt-spun at 18, 15, 9 and 3 m s^{-1}.

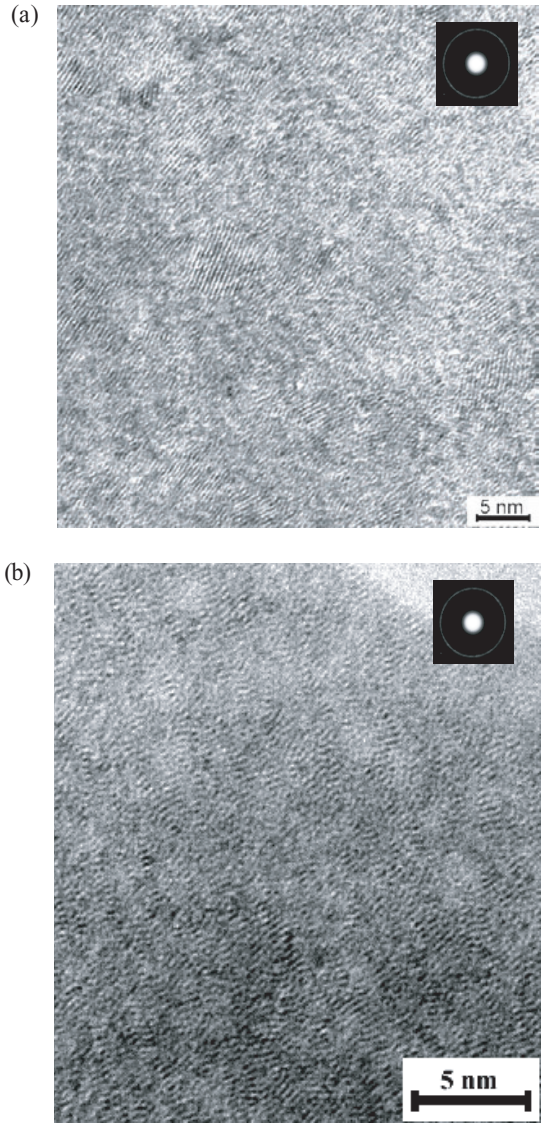

Figure 3. HRTEM images of (*a*) as-cast rod of 3 mm in diameter and (*b*) as-spun ribbon melt-spun at 15 m s^{-1}.

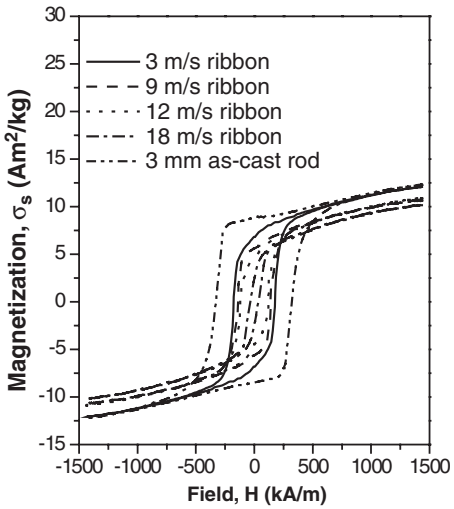

Figure 4. Hysteresis loops of melt-spun ribbons of various wheel speeds and as-cast rod of 3 mm in diameter.

4. Discussion

It is known that the precipitation of fine magnetic particles in the amorphous matrix can affect the magnetic properties of the material. The high coercivity in as-cast cylindrical sample is supposed to be attributed to the presence of a metastable highly anisotropic A1 phase or cluster. The interaction between these clusters has been proved to be existing in both samples on MFM observation [18, 22]. According to the random anisotropy model [19, 23], the alloy will exhibit high coercivity if the magnetic coherence length, which is equivalent to the dimension of the ordered clusters, is larger than the exchange length $L_{ex} = \sqrt{A/K}$ (A is the exchange stiffness and K is the crystal anisotropy constant). The exchange length L_{ex} could hardly be calculated because the structure of the clusters existing in both rod and ribbons is not very clear. The results of MFM experiments of the ribbons show that the coercivity H_c and the average size of the clusters D (depending on the quenching rate) roughly follow: $H_c \propto D^1$ due to the possible existence of a reduced exchange coupling [18]. Our recent EDS results on clusters in as-cast rod and as-spun ribbon have shown that the reduced exchange coupling might be coursed by the different composition of clusters in these two kind of samples. The ribbon annealed at low temperature possesses larger clusters with the same composition as that of in the as-cast rod and has much higher coercivity [25].

As to the formation of clusters, it can be understood from the equilibrium eutectic phase diagram. The DSC curves of crystalline $Nd_{60}Al_{10}Fe_{20}Co_{10}$ alloy show that the alloy is of near-eutectic composition. It is known that a primary phase will firstly crystallize from the melt of near-eutectic composition at an equilibrium state. A higher cooling rate may prevent the formation of primary phase and an extremely high cooling rate will prevent the crystallization of the alloy due to the depression of nucleation and growth. According to the nucleation theory, if the embryo surrounding possesses appropriate composition and structure similar to the chemical short-range-order (SRO) atom clusters existing in the supercooled melt, the nucleation is ready to occur due to the decrease of both nucleation energy [20]. But at a high cooling rate, the growth of the nuclei is almost impossible because it requires chemical redistribution and diffusion over longer distance and needs higher thermal activation energy. However, the eutectic alloys show a tendency of demixing processes prior to crystallization [24], the formation of a eutectic phase in $Nd_{60}Al_{10}Fe_{20}Co_{10}$ alloy which need lower activation energy might not be prevented completely, especially in such a deep eutectic alloy system. Thus, a metastable phase, i.e. cluster, will nucleate and grow based on the chemical SRO atoms due to the proper thermodynamical and structural conditions. As the nucleation rate and growth of the clusters are related to the diffusion of atoms, the amount and size of the clusters may increase with the lowering of the cooling rate. The irregular morphology of the clusters in as-spun ribbon (figure 3(*b*)) and the different composition of the clusters between as-cast rod and as-spun ribbon suggest the insufficiency of the diffusion time. The first exothermic reaction of the ribbons at about 473 K, which has been proved to be irreversible in DSC scan, ought to represent the relaxation of this irregular cluster structure.

5. Conclusions

In conclusion, clusters exist in the $Nd_{60}Al_{10}Fe_{20}Co_{10}$ metallic glass, although no obvious crystalline reflections are displayed in either the XRD or electron diffraction patterns. The magnetic properties and the crystallization behaviours of the Nd-rich metallic glasses are sensitive to the cooling rate. The coercivity increases gradually with the decreasing of cooling rate, which corresponds to the increasing of the size of the clusters.

Acknowledgments

The authors are grateful to the financial support of the National Nature Science Foundation of China (Grant Nos 50031010, 59971028, 59925101 and 10174088).

References

[1] Johnson W L 1999 *MRS Bull.* **24** 42
[2] Greer A L 1995 *Science* **267** 1947
[3] Inoue A 2000 *Acta Mater.* **48** 279
[4] Luborsky F E, Becker J J, Walter J L and Liebermann H H 1979 *IEEE Trans. Magn.* **15** 1146
[5] Jiang J Z, Sabel K and Rasmussen H 2001 *Appl. Phys. Lett.* **79** 1112
[6] Nagendra N, Ramamurty U, Goh T T and Li Y 2000 *Acta Mater.* **48** 2603
[7] Schroes J, Busch R and Johnson W L 2000 *Appl. Phys. Lett.* **76** 2343
[8] Shen T D and Schwarz R B 1999 *Appl. Phys. Lett.* **75** 49
[9] Wang W H, Wei Q and Bai H Y 1997 *Appl. Phys. Lett.* **71** 58
[10] Wang W H, Wei Q and Friedrich S 1998 *Phys. Rev.* B **57** 8211
[11] Inoue A and Zhang T 1997 *Mater. Sci. Eng.* A **226–228** 393
[12] Fan G J, Löser W, Roth S, Eckert J and Schultz L 1999 *Appl. Phys. Lett.* **75** 2984
[13] Inoue A, Zhang T, Zhang W and Takeuchi A 1996 *Mater. Trans., Jim.* **37** 99
[14] Inoue A, Takeuchi A and Zhang T 1998 *Metall. Mater. Trans.* A **29** 1779
[15] Fan G J, Löser W, Roth S, Eckert J and Schultz L 2000 *J. Mater. Res.* **15** 1556
[16] Li Y, Ng S C, Lu Z P, Feng Y P and Lu K 1998 *Philos. Mag. Lett.* **78** 213
[17] Wei B C, Wang W H, Pan M X, Han B S and Zhang Z R 2001 *Phys. Rev.* B **64** 012406
[18] Wei B C, Zhang Y, Zhuang Y X, Zhao D Q, Pan M X, Wang W H and Hu W R 2001 *J. Appl. Phys.* **89** 3529
[19] Xing L Q, Eckert J, Löser W, Roth S and Schultz L 2000 *J. Appl. Phys.* **88** 3565
[20] Fecht H J 1995 *Mater. Trans., Jim.* **36** 777
[21] Ding J, Si L, Li Y and Wang X Z 1999 *Appl. Phys. Lett.* **75** 1763
[22] Wei B C, Wang W H and Hu W R submitted
[23] Albert R, Becker J J and Chi M C 1978 *J. Appl. Phys.* **49** 1653
[24] Schneider S, Bracchi A, Samwer K, Seibt M and Thiyagarajan P 2002 *Appl. Phys. Lett.* **80** 1749
[25] Xia L, Wei B C, Wang W H and Dong Y D submitted